Valorization of Tunisian Pottery Clay onto Basic Dyes Adsorption

Bouatay, F.*, Dridi, S. and Mhenni, M.F.

Research Unit of Applied Chemistry & Environment, Department of Chemistry, Faculty of
Sciences, University of Monastir, Environment Street, 5019, Monastir, Tunisia

ABSTRACT: This study examined the adsorption behavior of two cationic dyes used in textile industries (CI Basic Red 46 and CI Basic Blue 3) on Tunisian clay used in pottery. The ability of pottery clay to remove the basic dyes from aqueous solution was compared to that of the commercial powdered activated carbon (PAC) and raw clay. Physicochemical characteristics of these adsorbents were performed by Boehm dosage, pH_{PZC} and CEC determination, particle size distribution and spectroscopic analysis (FTIR and UV-Vis). The pH_{PZC} of the pottery clay was about 9.86 and the CEC was about 15.6 meq/g. The empirical kinetic data fitted very well the pseudo second order model for the adsorbent studied. The isotherm data fitted rightly to the Langmuir isotherm model. The maximum adsorption capacities of the raw clay, pottery clay and PAC onto CI Basic Red 46 (CI Basic Blue 3) were respectively 2806 mmol/g (785 mmol/g), 2114 mmol/g (116.2 mmol/g) and 2123 mmol/g (343.9 mmol/g). These results showed the large adsorption capacities of the studied samples onto the basic dyes. Based on thermodynamic study, the adsorption of the cationic dye on raw clay, pottery clay and PAC appears to be physical adsorption process. The effect of the ionic strength study showed that the presence of electrolyte had an important effect on the basic dyes removal.

Key words: Pottery clay, Raw clay, Powdered activated carbon, Adsorption, Basic dyes

INTRODUCTION

There are more than 100000 types of dyes commercially available, with over $7*10^5$ tons of dyestuff produced annually. These dyes can be classified according to their structure as anionic and cationic products (Robinson *et al.*, 2001). In aqueous solution, anionic dyes carry a net negative charge due to the presence of sulphonate (SO_3^-) groups while cationic dyes carry a net positive charge due to the presence of protonated amine or sulfur containing group, and present a highly toxicity. (Netpradit *et al.*, 2004). In addition, dye wastewaters are commonly characterized by high salts content and low biodegradation potential (Alinsafi *et al.*, 2005) which makes effective removal by conventional wastewater treatment process difficult (Vimonses *et al.*, 2009). Therefore, removal of dyes is an important aspect of wastewater treatment before discharge. So, several effluent treatment methods have been used during the past years. These methods include: photo-catalytic degradation (Sohrabi *et al.*, 2008), sono-chemical degradation (Abassi *et al*, 2008), filtration (Saffaj *et al.*, 2005), cation exchange membranes (Wu *et al.*, 2009), electro-chemical degradation (Fan

et al., 2008), photo-Fenton (Nunez *et al.*, 2007), biological treatment (Lu *et al.*, 2009 ; Wang *et al.*, 2009), and adsorption (Errais *et al.*, 2012). Furthermore, it is difficult to remove basic dyes using chemical coagulation due to the high solubility in water. So, adsorption with activated carbon appears to be the best prospect for elimination of this dye. Despite the effectiveness, this adsorbent is expensive and difficult to regenerate after use. Moreover, there is a need to produce relatively cheap adsorbents that can be applied to water pollution control. Therefore, many researches in recent years have focused on the use of various low-cost adsorbents for dye removal from aqueous solution. Among these alternative adsorbents, it can be cited: carbonized organic material (Ho *et al.*, 2005), bagasse fly ash (Gupta *et al*, 2000), cellulose (Ben Douissa *et al.*, 2013), recycled alum sludge (Chu, 2001), sewage sludge (Dhaouadi *et al.*, 2009), earths (Atum *et al.*, 2003; Al Ghouti *et al*, 2003), agriculture residues (Lima *et al.*, 2008; Pavan *et al.*, 2008), fishery residues (Monvisade *et al.*, 2009; Crini *et al.*, 2008), microorganisms and also algae (Zakhama *et al.*, 2011).

Furthermore, clay minerals have a great potential to fix pollutants such as heavy metals, dye wastewater

*Corresponding author E-mail: bouatay_feriel@hotmail.com

and organic compounds, and they are widely applied in many fields of science and technology, for example, for the removal of liquid impurities and the purification of gases with surfactant-modified montmorilloniteas adsorbent agent(Juang *et al.*, 2002), or the dyes and surfactants from tannery waste waters with natural and acid-activated bentonite and sepiolite (Espantaleo *et al.*, 2003), due to their lamellar structure which provides high specific surface areas (Tsai *et al.*, 2004) and possibility to adsorb ions and polar organic molecules on particle external site and in interlayer positions (Gurses *et al.*, 2004). Basic Red 46 (BR 46) and Basic Blue 3 (BB3) were selected as a model synthetic azo dye due to their extensive use in textile industry. Azo dyes are a class of dyes characterized by the presence of the azo group. Due to high usage of these dyes, large volumes of colored effluents are discharged into environmental water sources. Their release into the environment is of concern due to their toxic, mutagenic and carcinogenic characteristics of the dyes and their biotransformation products. Hence, removal of azo dyes from wastewater is a major environmental issue. (Deniz and Karaman, 2011). In this regard, the aim of this study was to valorize the clay pottery waste in the waste water treatment. In this paper, the pottery wastes are used to remove a cationic textile dye. For the comparison, a multi-scale study, the PAC and the raw clay were used at the same time. The Basic Red 46 and the Basic Blue 3 were chosen as adsorbate in this work. The relevance of this work is to use both the macroscopic and microscopic data to understand the adsorption mechanism and to evaluate the dye removal.

MATERIALS & METHODS

The basic dyes used as adsorbate in the present study are C.I. Basic Red 46 (BR46) ($C_{19}H_{26}N_6O_4S$) and C.I Basic Blue 3 (BB3) ($C_{20}H_{26}N_3OCl$). These basic dyes are supplied respectively by Ciba and DyStar companies. The molecular mass of these dyes are respectively $M_r=$ 432g/mol and $M_r=359,45$g/mol. The molecular structures are shown in figure 1. The UV–vis spectra of the dyestuffs aqueous fraction were recorded using

a CECIL 2021 Instruments UV/Vis spectrophotometer and the results are represented in fig. 2. The maximum wavelengths λ_{max} of the dyes were found to be respectively 530nm and 580 nm.

Clays used in this research were collected from eastern Tunisia in the region of Monastir. The adsorbent studied in this paper were represented in figure 3. The samples were initially powdered, sieved (<60μm) and humidified at 20% water content and dried at 105°C for 24h. Then, the clay sample (S1) were powdered and passed through a 120 μm sieve. The sample noted S2 in this study was a waste pottery materiel which was a raw clay mixed with sand. This mixture was calcinated at 1000°C, powdered and passed through a 120μm sieve. The adsorption study of these clays materials onto the two basic dyes was compared to the adsorption behavior of the activated carbon (noted PAC: powdered activated carbon (commercialized)) onto these dyes.

The Boehm titration method was applied to determine the surface functional groups containing oxygen. The main principle of this method is that oxygen groups on carbon surfaces have different acidities and can be neutralized by bases of different strength. Prior to the analysis, samples were dried at 110°C for 3 h. Then, 0.5 g of each sample was added to glass bottles containing 25 ml of the following0.05M solutions: NaOH, $Na_2CO_3$and $NaHCO_3$. The bottles were sealed and shaken for 48 h to reach equilibrium. Then, the dispersions were filtered and 10 ml of the filtrates were pipetted to 100 ml Erlenmeyer flasks and the excess acid was back titrated with 0.05 M standard solutions of NaOH. The number of acidic sites was calculated assuming that NaOH neutralizes carboxylic, phenolic, and lactonic groups, Na_2CO_3 neutralizes carboxylic and lactonic groups, while $NaHCO_3$ neutralizes carboxylic groups only. (Milan *et al.*, 2011)

The point of zero charge (pH_{PZC}) of the studied sample was determined using the pH drift method. A stepwise addition of 0.1M HCl and/or 0.1M NaOH solutions were used for pH adjustment (3, 6 and 9).

(A)   **(B)**
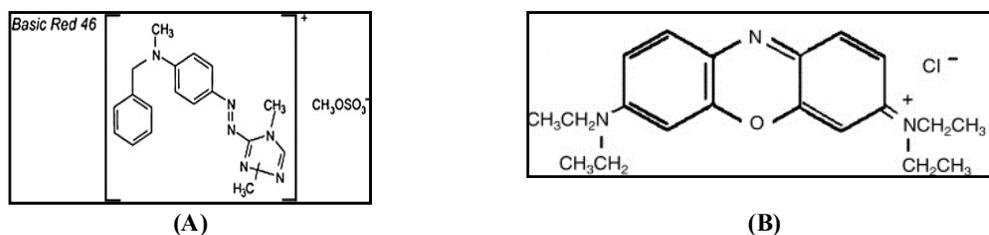
Fig.1. The chemical structure of basic dyes
(A) C.I Basic Red 46 (BR46); (B) C.I Basic Blue 3 (BB3)

(A)   (B)
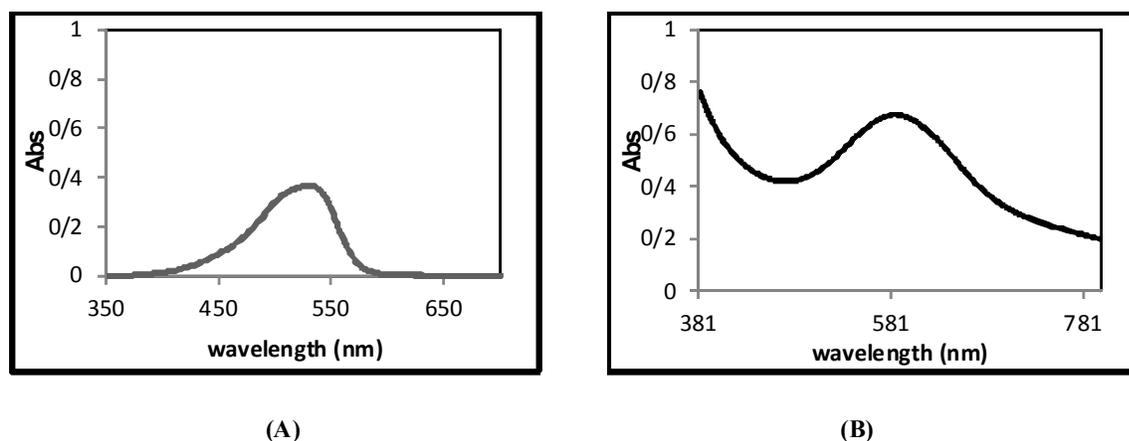
Fig.2. UV–vis spectra of basic dyes aqueous fractions
(A): BR 46 λmax=530 nm; (B) BB3 λmax=580 nm

A   **B**   **C**
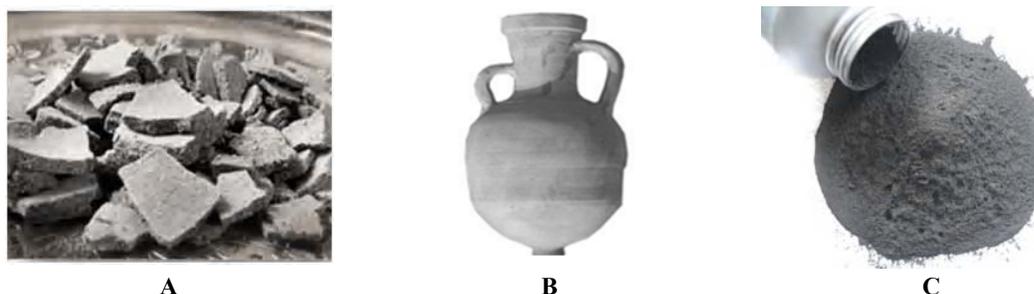
Fig.3. Description of studied adsorbents;
(A) : raw clay (S1) ; (B) pottery clay (S2); (C) powdered activated carbon (PAC)

0.05g; 0.1g; 0.5g; 1g; 2.5g and 5g of each sample were added to 100ml of NaCl (0.1M) at different pH. These solutions were shaken for 24h. Then, the dispersions were filtered and we measured the pH of the solution. The curves of the pH evolution with the samples mass were represented. The point of zero charge (pH_{PZC}) is the average of the three pH values reached constant depending on the mass. (Joong *et al*, 1990). The particle size distribution of studied samples was determined with wet separation method.(Alpha standard methods, 1999). The cation exchange capacity (CEC) of the studied sample were carried out by taking about 0.2 g of adsorbent (dried at 110°C) in a stoppered conical flask and added to it 25 ml 0.5 M $CaCl_2 \cdot 2H_2O$. It was shaken for 1 h in a shaker and allowed to settle overnight. The residue was filtered and washed with 75% methanol for 4-5 times, then washed with distilled water to free it from chloride. To the residue on filter paper, 30 ml 1 M KCl was added in parts for slow leaching. Finally the filtrate was titrated with 0.01 M

EDTA. The value of CEC was calculated from the amount of Ca^{2+} released (Barsha *et al.*, 2013).

Fourier transform infrared (FTIR) spectra were recorded on a Perkin–Elmer IR-197 spectrophotometer using potassium bromide disks. A total of 32 scans for each sample were taken with a resolution of 4/ cm, with a range of 4000–400/cm. The effect of the pH on the amount of the maximum adsorption capacities was studied over the pH range from 3 to 10. The pH was adjusted by adding a few drops of 0.5N of NaOH or 0.5N of HCl. In this study, 25ml of a fixed initial dye concentration at different pH were agitated with 0.075g of adsorbent using water bath shaker at 20°C. The agitation speed was provided at 150 rpm for 24h. The samples were centrifuged at 2000 rpm for 5min. The supernatant absorbance was measured using colorimetric method. The maximum adsorption capacities (q_e(mmol/g)) were determined according to equation Eq(1).

$$q_e(mmol/g) = \frac{(C_0 - C_f) \cdot V}{m} \tag{1}$$

Where C_0 and C_f are the initial and the final concentrations (mmol/L) of the dye solution, v (L) is the volume of the dye solution and m (g) is the clay sample. Adsorption kinetic experiments were carried out mixing 25ml of a constant dye concentration solution (at 20°C and pH= 6) (100 mg/l) with 0.075 g of adsorbent at the constant stirring speed of 150 rpm. Samples were centrifuged at 2000 rpm for 5min and the supernatant absorbance was measured using colorimetric method. In order to evaluate the effectiveness of an adsorbate, studies of kinetics of adsorption equilibria are also needed. Several kinetic models are available to examine the controlling mechanism of the adsorption process and to test the experimental data (Errais *et al.*, 2011). Four common kinetic models were tested: pseudo-first order, pseudo-second order, the Elovich and the Intraparticle diffusion models.

- The pseudo-first order equation

The pseudo-first order equation was used to fit the experimental results (Lagergren *et al.*, 1898).

$$q_t = q_e[1 - \exp(-K_1 t)] \tag{2}$$

Where q_e and q_t are the amounts of dye adsorbed per unit of adsorbent (mmol/g) at equilibrium time and time t, respectively, and K_1 (per min) is the rate constant for the first-order kinetics. The adsorption rate constant was determined from the plot of q_t against t.

- The pseudo-second order equation

The pseudo-second order model is expressed by equation Eq(3) (Chrayya *et al.*, 2004):

$$q_t = \frac{K_2 q_e^2 t}{1 + q_e K_2 t} \tag{3}$$

Where K_2 (per min) is the rate constant of adsorption, q_e is the amount of dye adsorbed at equilibrium (mmol/g) and q_t is the amount of dye adsorbed at time t (mmol/g).

- The Elovich equation

The Elovich equation is often used when the adsorbing surface is heterogeneous. The integration between time t=0 and t=t gives equation Eq(4)

$$q_t = \frac{1}{\beta} Ln(\alpha\beta) + \frac{1}{\beta} Ln(t) \tag{4}$$

Where α (mmol/g) is the initial adsorption rate constant and the parameter β (g/(mmol.min)) is related to the extent of surface coverage and activation energy for chemi-adsorptions.

- The Intraparticle diffusion equation

If the diffusion of dyes molecules on internal surfaces of pores and capillaries of the adsorbent is the rate-limiting step, the adsorption data can be presented by the following equationEq(5) (Yue *et al.*, 2011):

$$q_t = K_p t^{1/2} + C \tag{5}$$

Where K_p represents intraparticle diffusion rate constant (mmol/g/min$^{-1/2}$) and C is a constant (mmol/g) which gives information about the thickness of boundary layer.

Adsorption isotherm experiments were carried out mixing 25ml of an aqueous dye solution with different dye concentration (at 20°C and pH= 6) with 0.075 g of adsorbent at the constant stirring speed of 150 rpm for 24h. Samples were centrifuged at 2000 rpm for 5min and the supernatant absorbance was measured using colorimetric method.

In order to develop an equation which accurately represents the results and to establish the most appropriate correlations for the equilibrium data in the design of adsorption system, three common isotherm models were tested: Langmuir, Frendlich and Temkin models.

- Langmuir isotherm

The Langmuir adsorption model is based on the assumption that maximum adsorption corresponds to a saturated monolayer of solute molecules on the adsorbent surface. (Langmuir, 1918)

The Langmuir isotherm model is expressed by the following equation Eq(6):

$$\frac{C_e}{q_e} = \frac{1}{Q_m K_L} + \frac{1}{Q_m} C_e \tag{6}$$

Where q_e (mmol/g) is the amount of adsorbate per unit mass of adsorbent, C_e (mmol/L) is the equilibrium concentration of the adsorbate, Q_m (mmol/g) and K_L *(L/mmol)* are Langmuir constants related to adsorption capacity and rate of adsorption respectively and determined from the linear plot of specific adsorption (C_e/q_e) against the equilibrium concentration C_e.

.- Frendlich isotherm

The Frendlich isotherm (Frendlich, 1906) is the earliest known relationship describing the adsorption equation. The fairly satisfactory empirical isotherm can be used for non-ideal adsorption that involves heterogeneous adsorption and is expressed by the equation Eq(7):

$$q_e = K_F C_e^{1/n} \qquad (7)$$

Where K_F ($(mmol^{n-1/n} L^{1/n})/g$) is roughly an indicator of the adsorption capacity and 1/n is the adsorption intensity.

- Temkin isotherm

Temkin and Pyzhev, 1940, considered the effect of some indirect sorbate/adsorbate interactions on the adsorption isotherm. This isotherm assumes that; the heat of adsorption of all the molecules in a layer decreases linearly with surface coverage of adsorbent due to sorbate-adsorbate interactions. This adsorption is characterized by a uniform distribution of binding energies. The Temkin isotherm is expressed by the equation Eq(8)

$$q_e = \frac{RT}{b} [(Ln (AC_e)] \qquad (8)$$

The Equation (15) can be expressed in its linear form as the equation Eq(9):

$$q_e = B\, Ln\, A + B\, Ln\, C_e \qquad (9)$$

Where $B = \frac{RT}{b}$, T is the absolute temperature in K, R is the universal gas constant, A(mmol/L) is the

equilibrium binding constant and B (L/g) is related to the heat of adsorption..

The temperature is a parameter often investigated in literature and it is shown to affect the transport/kinetic process of dye adsorption (Gupta *et al*, 2006; Vimoses *et al*, 2009)

Therefore the dynamic activation parameters of the process such as enthalpy (ΔH), entropy (ΔS) and free energy (ΔG) of dye adsorption onto pottery clay were determined using the Eyring equation Eq(10) (Laidier and Meiser, 1999)

$$\log\left(\frac{q_e}{C_e}\right) = \frac{\Delta S_{ads}}{2,303R} - \frac{\Delta H_{ads}}{2,303RT} \qquad (10)$$

Where q_e is the amount of dye adsorbed per unit mass of samples (S1,S2, PAC) (mmol/g). C_e is the

equilibrium adsorbate concentration of dye in solution (mmol/L), T is temperature in Kelvin, and R is the gas constant.

The Gibb's free energy (ΔG_{ads}), entropy (ΔS_{ads}) and the enthalpy (ΔH_{ads}) changes for the adsorption were determined by equation Eq(11):

$$\Delta G_{ads} = \Delta H_{ads} - T\Delta S_{ads} \qquad (11)$$

The values of the enthalpy of adsorption (ΔH_{ads}) and the entropy of the adsorption (ΔS_{ads}) were determined from the slope and intercept of the linear plot of $\log\left(\frac{q_e}{C_e}\right)$ versus (1/T). Once ΔH_{ads} and ΔS_{ads} were obtained, ΔG_{ads} was determined from equation Eq(11).

The thermodynamic study was done only for the BR 46.

The effect of the electrolyte on the amount of the maximum adsorption capacities was studied by adding different electrolyte (Na_2CO_3, $CaCl_2$ and NaCl) in the dyeing solution (100 mg/L), and the electrolyte concentration were respectively 0.01M, 0.01M and 0.02M. In this study, 25 ml of a fixed initial dye concentration at different pH were agitated with 0.075g of adsorbent using water bath shaker at 20°C. The agitation speed was provided at 150 rpm for 24h. The samples were centrifuged at 2000 rpm for 5min. The supernatant absorbance was measured using colorimetric method. The dye removal (%) was determined from equation Eq(12).

$$Dye\ Removal\ (\%) = \frac{C_f}{C_0} * 100 \qquad (12)$$

Where C_0 and C_f are the initial and the final concentrations (mmol/L) of the dye solution.

Laboratory tests were conducted on effluent taken from a Tunisian dyeing and finishing of Denim Fabrics industry. Waste water characteristics were given in Table 1.The absorbance was measured using a CECIL 2021 Instruments UV/Vis spectrophotometer in the maximum wavelength ($\lambda_{max} = 630nm$).The chemical oxygen demand (COD) was measured according to the

Table 1. Industrial effluent characteristics

	Effluent
pH	11,9
Maximum wavelengths λ_{max}	630 nm
Abs	10,67
COD (mg O_2/L)	2350
Conductivity (mS/cm)	3,6
Turbidity (NTU)	38

Alpha standard method, 1999 and expressed as CODcr (potassium dichromate as oxidant). The turbidity was determined by a turbid-meter Turb 555IR according to the Alpha standard method. The adsorption tests were investigated at the same conditions described previously. Analysis of the decolorization and the chemical oxygen demand (COD) removal were carried out to evaluate the dyeing adsorption performance of the pottery clay onto industrial waste water. The decolorization (decolorization (%)) was measured using colorimetric method.

$$decolorization\ (\%) = \frac{Abs_i - Abs_f}{Abs_i} * 100 \quad (13)$$

Where Abs_i and Abs_f were the absorbance measured using a CECIL 2021 Instruments UV/Vis spectrophotometer in the maximum wavelength ($\lambda_{max} = 630nm$) of the effluent before and after adsorption, respectively.

The COD removal (%) was calculated according to equation Eq(14):

$$CODremoval(\%) = \frac{COD_i - COD_f}{COD_i} * 100 \quad (14)$$

Where $COD_i (mgO_2/L)$ and $COD_f (mgO_2/L)$ were, respectively, the chemical oxygen demands of the effluent before and after the coagulation-flocculation treatment.

RESULTS & DISCUSSION

The PZC was measured for the clay samples. The results are presented in Table 2. The pH at which the total particle charge is zero, is called the point of zero charge (PZC), which is one of the most important parameters used to describe variable-charge surfaces (Al Des *et al.*, 2003; Casttilla, 2004; Nabais *et al.*, 2011). The pH_{PZC} characterized the acidity or the alkalinity of the surface. A pH lower than the pH_{PZC}, the surface charge was positive (acidity) and a pH higher than the pH_{PZC}, the surface charge was negative (alkalinity) and tends to decrease. The pH_i of the dye bath was about 5,5. So the clay samples have a higher value of pH_{PZC} than dye bath pH ($pH_{PZC} >> pH_i$), so the surface charges of the sorbent are positive. The cation exchange capacity (CEC) values were given in Table 2. CEC values vary from 15meq/g to 15.6meq/g. The lowest CEC was obtained for the raw clay (S1). The particle size distribution of the clay samples and PAC was represented in Table 3. The highest percentage of size particle was varied from 20 to 63 μm. The raw clay presented the highest percentage of the smaller particle (<2μm) and the highest dye removal. The particle size of adsorbent inversely influences the adsorption process. Smaller the particles, higher the adsorption efficiency and capacity due to large total surface area of the adsorbent (Safa and Bhati, 2011). Asgher and Bhatti, 2012, also observed non significant increase in adsorption capacity of bio-adsorbents when particle size was reduced from 1000 μm to 250 μm. Nassar *et al.*, 2012, also reported that 80% reduction in the particle size could increase the adsorption capacity of clay by 7.8%. Based on these facts, it is assumed that adsorption parameters improve up to certain particle size and then, remains constant.

Table 4 summarized the results of Boehm titration and showed that most of acidic functional groups are carboxylic, followed by lactonic and phenolic for the studied clay samples. The effect of the initial pH values for the adsorption of BR46 and BB3 dyes in solution onto raw and pottery clays was investigated in the range of pH 3-12 and given in fig. 4. The PZC measured for the sample used vary from 8.68 to 10.1. The adsorption capacity of BR46 and BB3 onto the studied clays increased significantly when the pH of dye solution increased from 10.1 to 12. This means that the charge sign on the surface of the clay remains negative in a wide pH range (10.5–12). When the solution pH is basic, the negative charged clay surface favors the BR46 and BB3 adsorption.

Table 2. Surface properties of clays

	CEC (meq/g)	PZC
S1	15	8,68
S2	15,6	9,86
PAC	15,4	10,1

Table 3. The size distribution of the sample (%)

Sieve size	S1	S2	PAC
>to 100 μm	9,98	27,4	0
From 100 to 90 μm	2,59	8,6	0,012
From 90 to 63 μm	3,85	18,34	5,8
From 63 to 20 μm	82,11	45,82	87,54
From 20 to 2 μm	1,44	0,6	6,7
< 2 μm	0,02	0,012	0,02

Table 4. The acidic functional groups of studied samples

Sites number (10^{20}/g of adsorbent)	S1	S2	PAC
Carboxylic	10,24	9,037	13,407
Lactonic	8,736	5,723	6,928
Phenolic	13,7	1,43	2,711

Table 5. The kinetic parameters of BR46 dye adsorption

	Pseudo first order			Pseudo second order			Elovich			Intraparticule diffusion		
	q_e	K_1	R^2	q_e	K_2	R^2	α	β	R^2	K_p	C	R^2
S1	68.7	0.254	0.996	67.96	1.018	0.996	55708	0.17	0.93	0.918	53.51	0.44
S2	43.26	0.46	0.951	44.23	0.072	0.954	57761	0.15	0.64	0.763	32.96	0.67
PAC	56.43	0.47	0.954	57.54	0.062	0.956	12706	0.23	0.1	1.087	42.47	0.78

Table 6. The kinetic parameters of BB3 dye adsorption

	Pseudo first order			Pseudo second order			Elovich			Intraparticule diffusion		
	q_e	K_1	R^2	q_e	K_2	R^2	α	β	R^2	K_p	C	R^2
S1	89.52	0.393	0.999	90.97	0.118	0.999	5.035	0.5	0.10	0.89	71.69	0.11
S2	67.65	0.056	0.948	79.34	0.0024	0.97	111.28	0.04	0.87	1.64	37.94	0.51
PAC	78.53	0.142	0.979	85.99	0.0083	0.994	106836	0.086	0.80	1.19	57.83	0.24

Table 7. The isotherm parameters of BR46 dye adsorption

	Langmuir			Frendlich			Temkin		
	Q_m	K_L	R^2	K_F	n	R^2	A	B	R^2
S1	2805	0.00138	0.978	46.49	2.0133	0.974	1.287	267.67	0.84
S2	2114	0.00018	0.995	0.519	1.099	0.985	0.911	225.23	0.702
PAC	2123	0.00055	0.991	6.39	1.447	0.990	0.262	151.93	0.706

Table 8. The isotherm parameters of BB3 dye adsorption

	Langmuir			Frendlich			Temkin		
	Q_m	K_L	R^2	K_F	n	R^2	A	B	R^2
S1	785.36	0.0064	0.942	47.23	2.9	0.82	0.598	121.54	0.893
S2	116.2	0.0434	0.76	39.29	8.06	0.43	3.316	43.07	0.718
PAC	343.92	0.0274	0.867	64.63	5.04	0.63	11.35	12.76	0.513

Therefore, the amount of BR46 and BB3 adsorbed on the clay tended to decrease with the decrease of pH, which can be attributed to the electrostatic repulsion between the positively charged surface and the positively charged dye molecule for pH below 10.5. Also, the lower adsorption of BR46 and BB3 at acidic pH may be due to the presence of excess H^+ ions competing with dye cations for the adsorption sites. These observations were similar to those findings by other workers. (Tahir and Rauf, 2006; Selvan *et al*, 2008). For further adsorption studies, the dye solution pH's were adjust at pH 6.0, which is approximately equal to natural aqueous dye solution pH. The parameters calculated for the different models are given in Tables5 and 6. The kinetic study of the BR 46 and BB3 basic

dyes onto the raw clay (S1), pottery clay (S2) and powdered activated carbon (PAC) were determined in the same conditions. The kinetic data obtained gave poor fits with, Elovich and intraparticle diffusion models. But a good fit was obtained with the pseudo first order and the pseudo second order model as shown by the high correlation coefficient (R^2 vary from 0.999 to 0.948). A comparison of these results with the experimental suggests that the second order model is more reasonable than the first order one. The kinetic curves were represented for the second order model in figures 5 and 6, suggesting that the adsorption involve more than one step. Consequently, the adsorption can be governed by chemical process involving cations exchange. The dye removal was rapid in the initial stage of contact time and reached equilibrium already after 10
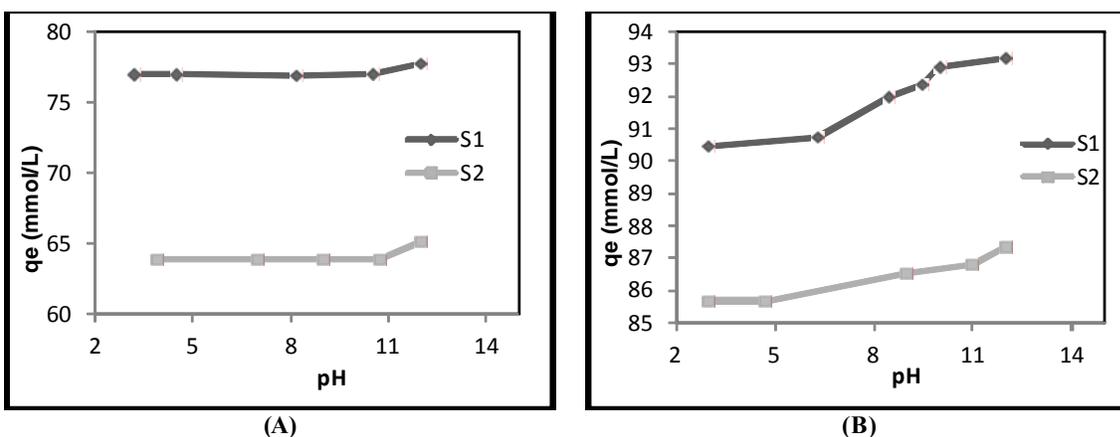
**Fig.4. The pH effect of the raw clay (S1) and pottery wastes (S2) for the adsorption of basic dyes
(A): BR 46; (B):BB3**
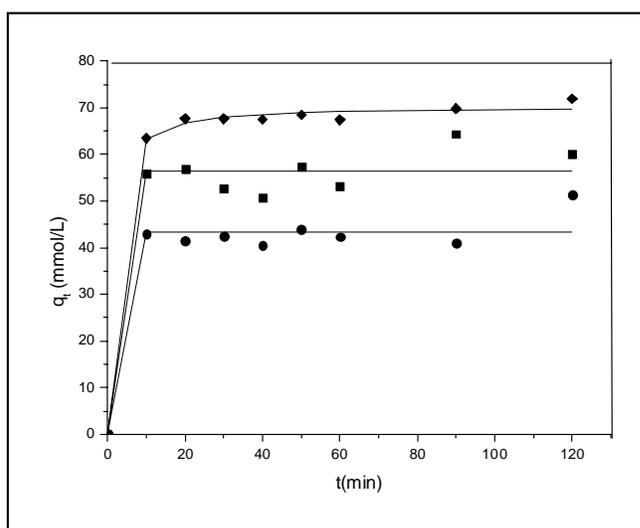
Fig.5. The kinetic curves of BR46 retention by adsorbent materials:

♦ raw clay(S1), ●pottery clay (S2) and ■ PAC

min for the different adsorbents, this explain the low value of the correlation coefficient of the intraparticle diffusion model. The rapid adsorption during the first 10 min was probably due to the abundant availability of actives sites on the adsorbent surface, but with the gradual occupancy of these sites, the adsorption became less efficient. These results showed that for the same initial mass of the adsorbent and dye concentration, the adsorption rate was very important for the raw clay, PAC and pottery clay (respectively 67.96mmol/g; 44.23mmol/g; 57.54mmol/g) for the BR46 and 90.96mmol/g; 79.34mmol/g and 85.99mmol/g for the BB3. At the chosen experimental conditions, the adsorbent with the lowest cation exchange capacities (CEC for S1=15 meq/g) possessed the highest adsorption rate

and yield. Therefore, the exchange phenomenon between the layers were probably responsible of the adsorption processes what was to be expected considering the negative surface charge of the adsorbent and the cationic nature of dye molecule. The parameters of the isotherm calculated for the different models were given in Tables7 and 8.The isotherm data gave a good fit with Langmuir model as shown by the highest correlation coefficient (R^2 vary from 0.995 to 0.76). A comparison of these results with the experimental showed that the Langmuir model is more reasonable than the Frendlich and Temkin model. For the Langmuir model, the plot of the adsorption rate q_e(mmol/g) against the equilibrium concentration (C_e (mmol/L)) was represented in figs7 and 8.

The best equilibrium model was determined based on the regression correlation coefficient R^2. From Tables 7 and 8, it was observed that the equilibrium adsorption data were very best represented by the Langmuir isotherm. The best fit isotherm expressions confirm the monolayer coverage process of BR46 and BB3 onto clay and PAC samples.

Tables 7 and 8 list a comparison of maximum monolayer adsorption capacity of BR46 (BB3) on raw clay, pottery clay and PAC. The raw clay and the pottery clay are found to have a relatively large adsorption capacity of 2806mmol/g (785mmol/g) and 2114mmol/g (116.2mmol/g) respectively, and this indicates that clay could be considered a promising material for the removal of BR46 (BB3) from aqueous solution, mostly when compared with activated carbon (PAC) 2123mmol/g (343.9mmol/g). A comparison of the adsorption capacities of different sorbents for basic dyes is given in Table 9. Infrared spectroscopy was applied to clay materials, to differentiate between the molecules of water hydration and formation of hydroxyl groups and followed the structural changes after firing the raw material. The IR spectroscopy of the raw clay and pottery clay before and after adsorption of BR46 were represented respectively in figs 9 and 10. The IR spectrum of raw clay (dried at 105°C) is used as a reference for interpreting any possible structural changes in different experimental conditions. The vibration bands (Al-OH-Al) valence to 3620/cm and deformation at 915/cm in the spectrum of the sample (S1) indicates that the raw clay is dioctahedral. (Paletha *et al.*, 2005). The deformation band in 1630/cm is characteristic of the water hydroxyl vibrations in the raw clay. These vibrations are present only for the raw clay and they disappear for the treated

Table 9. The maximum sorption capacities (mmol/g) of basic dyes of various sorbents

Basic dyes	Absorbent	Qm (mmol/g)	Kinetic	Isotherm	References
Basic Red 46	Moroccan Clay	125	Pseudo-second order	Langmuir	Benneni *et al*, 2009
Basic Red 46	Regenerated Clay	169	Pseudo-second order	Langmuir	Mezitia and Boukerroui, 2012
Basic Red 46	Pine tree leaves	166.52	Pseudo-second order	Langmuir	Deniz and Karaman, 2011
Brillant Green	Kaolin	139.28	Pseudo-second order	Langmuir	Nandi *et al*, 2009
Crystal Violet	Kaolin	115.85	Pseudo-second order	Langmuir	Nandi *et al*, 2009
Methylene Blue	Montmorillonite Clay	903.54	Pseudo-second order	Langmuir	Almeida *et al*, 2009
Methylene Blue	Activated Clay	340.78	Pseudo-second order	Langmuir	Weng *et al*, 2005
Basic Red 46	pottery Clay	2114	Pseudo-second order	Langmuir	Present study
Basic Blue 3	Pottery clay	116,2	Pseudo-second order	Langmuir	Present study
Basic Red 46	Tunisian Clay	2806	Pseudo-second order	Langmuir	Present study
Basic Blue 3	Tunisian clay	785	Pseudo-second order	Langmuir	Present study
Basic Red 46	PAC	343.9	Pseudo-second order	Langmuir	Present study
Basic Blue 3	PAC	2123	Pseudo-second order	Langmuir	Present study

Table 10. The thermodynamic parameters

	ΔH (KJ/mol)	ΔS (J/mol)	$\Delta G_{20°C}$ (KJ/mol)	$\Delta G_{40°C}$ (KJ/mol)	$\Delta G_{60°C}$ (KJ/mol)
S1	-1,582	1,474	-2,013	-2,043	-2,073
S2	26,022	82,1	1,966	0,324	-1,317
PAC	-50,704	-138,42	-10,146	-7,378	-4,616
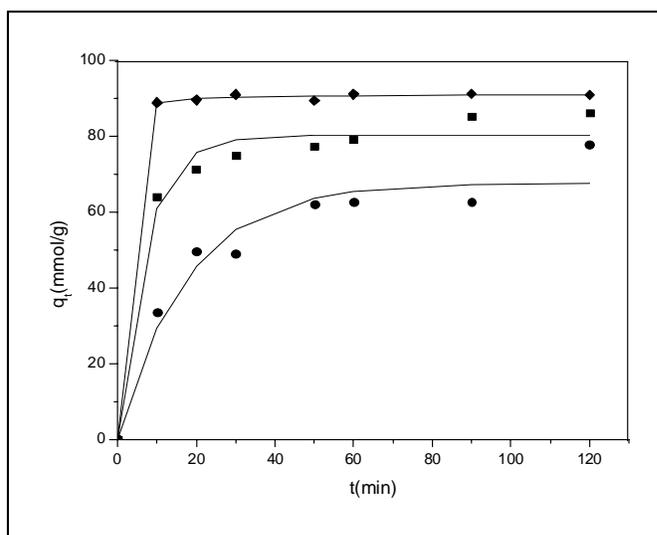
Fig.6. The kinetic curves of BB3 retention by adsorbent materials:
♦ raw clay(S1), •pottery clay (S2) and ■ PAC
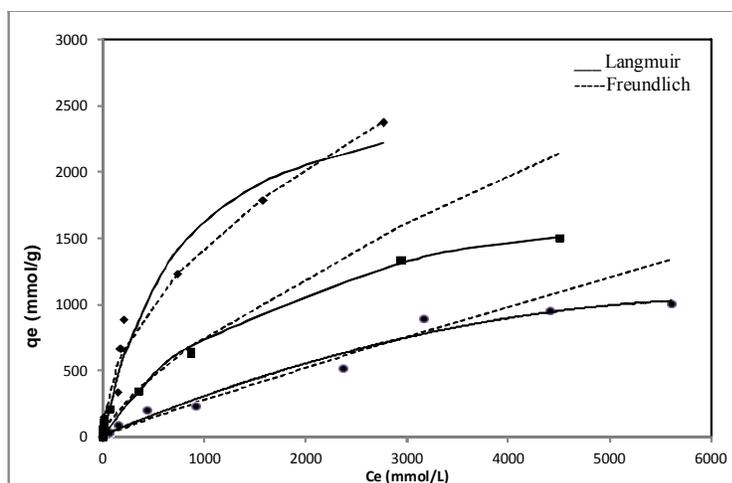
Fig.7. The isotherm curves of BR46 retention by adsorbent materials:
♦ raw clay(S1), •pottery clay (S2) and ■ PAC

samples. The strong bands at 1100 and 1000/cm are characteristic of stretching vibrations of (Si-O) in the plane and out of plane. It should be noted that the intensity of the band at 1000/cm decreases for the pottery clay (fired at 1100°C), corresponding to the stretching vibrations of the silica. This reflects the formation of tetrahedral bonds (Si-O-Si) from the amorphous silica (Si-O). The stretching vibrations between 650/cm and 950/cm contain area of absorbing vibration characteristics of phyllosilicates at 910/cm and Al-O at 720-780/cm.

After dyeing adsorption the IR spectrum of the raw clay presents modification in the vibrations stretching between 1200/cm and 1700/cm, and the intensity of the vibration bonds at 1000/cm was varied

for the clays fired at different temperature. The thermodynamic parameters of adsorption based on the above functions are listed in table 10. The raw clay and the PAC presented negative values of enthalpy (ΔH_{ads}) and free energy (ΔG_{ads}). The negative values of ΔH_{ads} indicate that the process of adsorption of these materials is exothermic in nature, and the negative values of ΔG_{ads} show the spontaneous adsorption of cationic dye on the adsorbent. But, ΔG_{ads} is less negative for the PAC and more negative for raw clay with temperature increase. It shows that the adsorption process is thermodynamically feasible at room temperature but less with high temperature. Physical adsorption and chemical-adsorptions can be classified, to a certain extent, by the magnitude of the enthalpy change. It is accepted that the bonding strength of <84
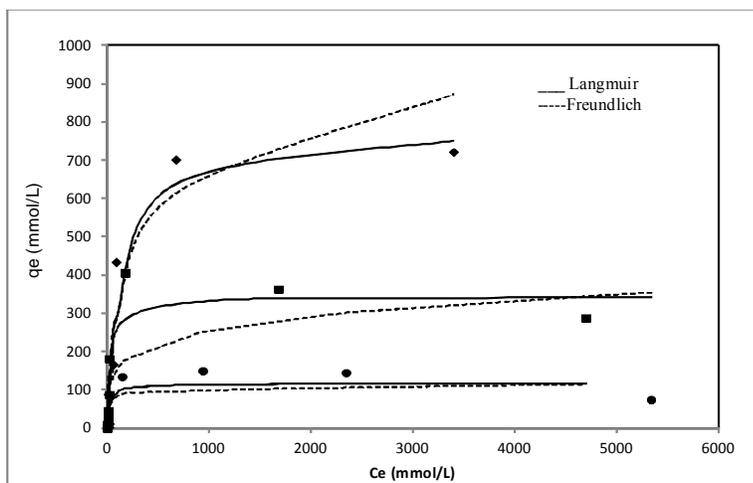
Fig. 8. The isotherm curves of BB3 retention by adsorbent materials:

♦raw clay(S1), •pottery clay (S2) and ■ PAC
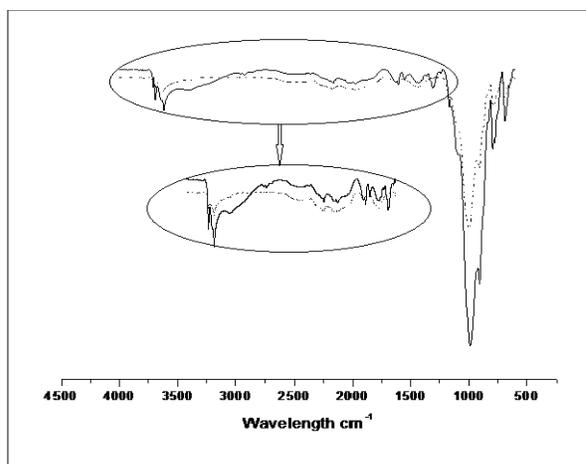
Fig.9. IR Spectrum of raw clay before and after BR46 adsorption (— before adsorption, – after adsorption)
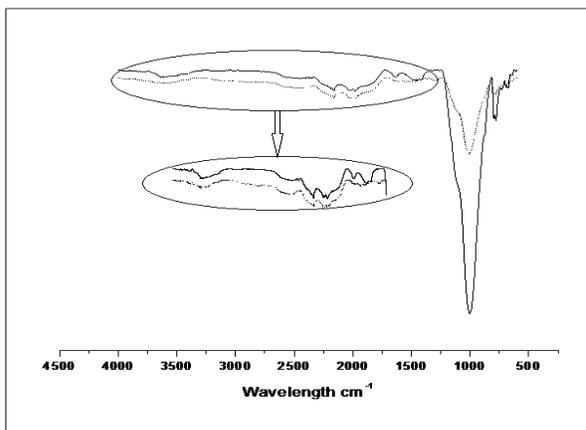
Fig.10. IR spectrum of pottery clay before and after BR46 adsorption (— before adsorption, – after adsorption)
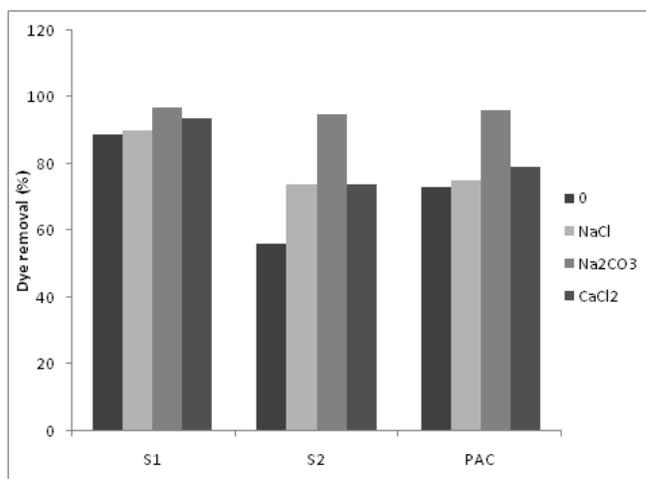
Fig.11. The effect of electrolyte on dye removal for BR46

KJ/mol are typically those of physical adsorption type bonds. Chemical-adsorption bond strengths can range from 84 to 420 KJ/mol(Faust and Aly, 1987). Based on this, the adsorption of the cationic dye BR 46 on raw clay, pottery clay and PAC appears to be physical adsorption process. The effect of the ionic strength was determined in the same operating conditions for different adsorbent. The dye removal of the BR46 and BB3 are represented respectively in figure 11 and 12. The results showed that the presence of different electrolyte (NaCl, Na_2CO_3 and $CaCl_2$) on dyes removal efficiency. The presence of the electrolytes increases the dye removal efficiency to some extent and this behavior is more notable for the BB3 than the BB46. The dye removal was the highest with the presence of the Na_2CO_3 and the lowest for the presence of NaCl for both the BR46 and BB3. The presence of the electrolyte may have two different effects in the opposite direction. First, they may cause the neutralization of surface charge of adsorbent while competing with dye for the surface adsorption (Tehrane-Bayha *et al.*, 2011). With the increasing ionic strength, the adsorption capacity decreases due to the screening of the surface charges (Nandi *et al.*, 2009). The performance of the pottery clay for the adsorption of industrial dyeing effluent was investigated. This effluent was taken from Tunisian dyeing and finishing industry of DENIM fabrics. The waste water contains dyes, chemical substances and auxiliaries used in the dyeing and finishing processes. COD and color were measured before and after adsorption. The color and the COD removal of the industrial waste water were given in figure 13. The results showed that the removal percentage of real effluent on pottery clay was significant. It initial COD (2350 mgO_2/L) decreased down to 1097 mgO_2/L with a COD removal percentage of 53.31% after 2h of adsorption. Meanwhile, the solution color decreased by 57.9%.

CONCLUSIONS

The pottery clay materials were used in Tunisian to conserve water and oil. The pottery clay wastes were valorized in this paper for basic dyes removal. This paper showed that this low cost material presented a large adsorption capacity. The adsorption behavior of this non conventional material was compared to that of the raw clay and powdered activated carbon. The adsorption mechanism depends on the effluent pH and the ionic strength. This paper developed the pH effect and the influence of the ionic strength on the adsorption capacities of basic dyes onto the pottery clay. The kinetic modeling study has shown that the experimental data were found to follow the pseudo second order model. Furthermore, the isotherm data agreed well with Langmuir model for the raw clay, pottery clay and PAC onto CI Basic Red 46 (CI Basic Blue 3) with adsorption capacities of 2806 mmol/g(785 mmol/g), 2114mmol/g (116.2mmol/g) and 2123mmol/g (343.9 mmol/g) respectively. Besides, the adsorbent characterization and the thermodynamic study showed that the adsorption of the cationic dyes on raw clay, pottery clay and PAC appears to be physical adsorption process.

REFERENCES

Abbasi, M. and RazzaghiAsl, N. (2008). Sonochemical degradation of Basic Blue 41 dye assisted by nanoTiO$_2$ and H$_2$O$_2$. Journal of Hazardous Materials, **153 (3)**, 942–947.

Al Degs, Y., Khaisheh, M.A.M, Allen, S. J. and Ahmed, M. N. (2003). Effect of carbon surface chemistry on the removal reactive dyes from textile effluent. Water Research, **34**, 927-935.

Al Ghouti, M. A., Kraisheh, M.A.M., Jallen, S. and Ahmad, M.N. (2003). The removal of dyes from textile waste water: a study of physical characteristics and adsorption mechanism of diatomaceous earth. Journal of Environmental Management, **69**, 229-238.

Alinsafi, A., Khemis, M., Pons, M. N., Leclerc, J. P., Yaacoubi, A., Benhammou, A. and Nejmeddine A. (2005). Electro-coagulation of reactive textile dyes and textile wastewater, Chemical Engineering and Processing: Process Intensification, **44 (4)**, 461–470.

Almeida, C. A. P., Debacher, N. A., Downs, A. J., Cotteta, L. and Mello, C. A. D. (2009). Removal of methylene blue from colored effluents by adsorption on montmorillonite clay. Journal of Colloid and Interface Science, **332**, 46–53.

APHA, (1999). Standard Methods for the Examination of Water and Wastewater, 20th ed.,American Public Health Association (APHA), AWWA, WEF, Washington, DC, USA.

Asgher, M. and Bhatti, H. N. (2012). Evaluation of thermodynamics and effect of removal of anionic dyes from aqueous solution. Ecological Engineering, **38**, 79-85.

Atum, G., Hisarli, G., Sheldrich, W.S and Muhler, M. (2003). Adsorptive removal of methylene blue from colored effluents bon fuller's earth, Journal of colloid and interface science, **261**, 32-39.

Baruah, B., Mishra, M., Bhattacharjee, C. R., Nihalani, M.C., Mishra, S. K., Baruah, S. D., Phukan, P. and Goswamee, R. L. (2013). The effect of particle size of clay on the viscosity build up property of mixed metal hydroxides (MMH) in the low solid-drilling mud compositions. Applied Clay Science, **80–81**, 169–175.

Ben Douissa, N., Bergaoui, L., Mansouri, S., Khiari, R. and Mhenni, M. F. (2013). Macroscopic and microscopic studies of methylene blue adsorption onto extracted celluloses from Posidonia oceanic, Industrial Crops and Products, **45**, 106–113

Bennani, A. K., Mounira, B., Hachkara, M., Bakasse, M. and Yaacoubi, A. (2009). Removal of Basic Red 46 dye from aqueous solution by adsorption onto Moroccan clay. Journal of Hazardous Materials, **168**, 304–309.

Bhatacharyya, K. G. and Sharma, A. (2004). AzardirachtaIndica leaf powder as an effective biosorbent for dyes: a case study with aqueous Congo red solution, Journal of Environmental Management, **71**, 217–229.

Casttilla, M. (2004). Adsorption of organic molecules from aqueous solutions on carbon materials. Carbon, **42**, 83-94.

Chu, W. (2001). Dye removal from textile dye waste water using recycled alum sludge, Water Research, **35**, 3147-3152.

Crini, G., Gimbert. F., Robert. C., Martel, B., Adam, O., Morin-Crini, N., De Giorgi, F. and Badot, P. M. (2008), The removal of Basic Blue 3 from aqueous solutions by chitosan-based adsorbent: Batch studies, Journal of Hazardous Materials, **153**, 96–106.

Deniz, F. and Karaman, S. (2011). Removal of Basic Red 46 dye from aqueous solution by pine tree leaves. Chemical Engineering Journal, **170 (1)**, 67–74.

Dhaouadi, H. and M'Henni, F. (2009). Vat dye adsorption onto crude dehydrated sewage sludge, Journal of Hazardous Materials, **164**, 448–458.

Elovich, S. J. (1959). Proceedings of the Second International Congress on Surface Activity. 11, in: J.H. Schulman (Ed.), Academic Press, Inc, New York, 253.

Errais, E., Duplay, J., Darragi, F., M'Rabet, I., Aubert, A., Huber, F. and Morvan, G. (2011). Efficient anionic dye adsorption on natural untreated clay: Kinetic study and thermodynamic parameters. Desalination, **275**, 74–81.

Errais. E., Duplay, J., Elhabiri, M., Khodjac, M., Ocampod, R., Baltenweck-Guyote, R. and Darragif, F. (2012). Anionic RR120 dye adsorption onto raw clay: Surface properties and adsorption Mechanism. Colloids and Surfaces A: Physicochemical and Engineering Aspects, **403**, 69-78.

Espantaleon, A.G., Nietoa, J. A., Fernandez and M., Marsal. (2008). Use of activated clays in the removal of dyes and surfactants from tannery waste waters. Applied Clay Science, **24**, 105 – 110.

Fan, L., Zhou, Y., Yang, W., Chen, G. and Yang, F. (2008). Electrochemical degradation of aqueous solution of Amaranth azo dye on ACF under potentiostatic model. Dyes and Pigments, **76 (2)**, 440–446

Faust, S. and Aly, O. (1987). Adsorption processes for water treatment, Butter worth Publishers.

Freundlich, H. M. (1906). Uber die adsorption in lösungen. ZeitschriftfürPhysikalischeChemie, **57**, 385-470.

Gupta, V. K, Mohan, D. and Saini, V. K. (2006), Studies on the interaction of some azo dyes (naphtol red J and Direct Orange) with montorinite mineral. Colloidal Interface Science, **298**, 79-86.

Gupta, V. K., Mohan, D., Sharma, S. and Sharma, M. (2000). Removal of basic dyes (rhodamine B and methylene blue) from aqueous solutions using bagasse fly ash. Separation Science Technology, **35**, 2097–2113.

Gürses, A., Karaca, S., Doar, Ç.,Bayrak, R., Açýkyýldýz, M. and Yalçýn, M. (2004). Determination of adsorptive properties of clay/water system: methylene blue adsorption. Journal of Colloid and Interface Science, **269**, 310–314.

Hameed, B. H., Mahmoud, D. K. and Ahmad, A. L. (2008). Adsorption equilibrium and kinetics of basic dye from aqueous solution using banana stalk waste. Journal of Hazardous Materials, **158**, 499–506.

Ho, Y. S., Chiu, W. T. and Wang, C. C. (2005). Regression analysis for the adsorption isotherms of basic dyes on sugarcane dust. Bioressource Technology, **96**, 1285-1291.

Joong, S., Schwarz, J. A. (1990). Effect of HNO_3 treatment on the surface acidity of activated carbons. Department of Chemical Engineering and Materials Science, Syracuse University, Syracuse, NY 13244.

Juang, R. S., Lin, S. H. and Tsao, K. H. (2002). Mechanism of Adsorption of Phenols from Aqueous Solutions onto Surfactant-Modiûed Montmorillonite. Journal of Colloid and Interface Science, **254,** 234–241.

Lagergren, S. (1898). About the theory of so-called adsorption of soluble substances. KungligaSuenk, Vetenskapsakademiens, Handlinger Band. **24,** 1–39.

Laidier, K. J. and Meiser, J. M. (1999). Physical chemistry, Houghton Mifflir New York, 852.

Langmuir, L. (1918). The adsorption of gases on plane surfaces of glass, mica and platinum. Journal of American Chemistry, **57**, 1361-1403.

Lima, E. C., Royera, B., Vaghetti, J. C. P., Simon, N. M., Da Cunha, B. M., Pavan, F. A., Benvenutti, E. V., Cataluna-Veses, R. and Airoldi, C. (2008). Application of Brazilian pine-fruit shell as a biosorbent to removal of reactive red 194 textile dye from aqueous solution Kinetics and equilibrium study. Journal of Hazardous Materials, **155**, 536–550

Lu, X., Yang, B., Chen, J. and Sun, R. (2009). Treatment of wastewater containing azo dye reactive brilliant red X-3B using sequential ozonation and upflow biological aerated filter process. Journal of Hazardous Materials, **161 (1)**, 241–245.

Mezitia, C. and Boukerroui, A. (2012). Removal of a Basic Textile Dye from Aqueous Solution by Adsorption on Regenerated Clay. Procedia Engineering, **33**, 303 – 312.

Milan, M., Purenoviæ, M., Bojiæ, A., Zarubica, A. and Ranðeloviæ, M. (2011). Removal of lead(II) ions from aqueous solutions by adsorption onto pine cone activated carbon. Desalination, 276, 53–59.

Monvisade, P. and Siriphannon, P. (2009). Chitosan intercalated montmorillonite: Preparation, characterization and cationic dye adsorption. Applied Clay Science, **42 (3–4)**, 427–431.

Nabais, J. M. V., Eduardo, C, Langinhas, C., Carrott, P. J. M. and RibeiroCarott, M. M. L. (2011). Production of activated carbons from almond shell. Fuel Processing Technology, **92,** 234-240.

Nandi, B. K., Goswami, A. and Purkait, M. K. (2009). Removal of cationic dyes from aqueous solutions by kaolin: Kinetic and equilibrium studies. Applied Clay Science, **42**, 583–590

Nassar, M. N., El Geundi, M. S and Alwahbi, A. (2012). Equilibrium modeling and thermodynamic parameters for adsorption of cationic dyes onto yemen natural clay. Desalination Water Treatment, **44**, 340-349.

Netpradit, S., Thiravetyan, P. and Towprayoon, S. (2004). Adsorption of three azo reactive dyes by metal hydroxide sludge: effect of temperature, pH, and electrolytes. Journal of Colloid and Interface Science, **270 (2)**, 255–26.

Núñez, L., Antonio, J., Hortal, G. and Torrades, F. (2007). Study of kinetic parameters related to the decolorization and mineralization of reactive dyes from textile dyeing using Fenton and photo-Fenton processes. Dyes and Pigments, **75 (3)**, 647–652.

Pavan, F. A., Lima, E. C., Dias, S. L. P. and Mazzocato, A. C. (2008). Methylene blue bioadsorption from aqueous solutions by yellow passion fruit waste. Journal of Hazardous Materials, **150 (3)**, 703–712.

Push Paletha, P., Rugmini, S. and Lalithambika, M. (2005). Correlation between surface properties and catalytic activity of clay catalysts. Applied Clay Science, **30,** 141-153.

Robinson, T., McMullan, G., Marchant, R. and Nigam, P. (2001). Remediation of dyes in textile effluent: a critical review on current treatment technologies with a proposed alternative. Bioresource Technology, **77**, 247-255.

Safa, Y. and Bhatti, H. N. (2011). Kinetic and thermodynamic modeling for the removal of Direct Red 31 and Direct Orange 26 dyes from aqueous solution by rice husk. Desalination, **272**, 313-322.

Saffaj, N., Persin, M., AlamiYounssi, S., Albizane, A., Bouhria, M., Loukili, H., Dach, H. and Larbot, A. (2005). Removal of salts and dyes by low $ZnAl_2O_4$–TiO_2 ultrafiltration membrane deposited on support made from raw clay. Separation and Purification Technology, **47 (1-2)**, 36–42.

Selvan, P., Prathe, S., Basakaralingram, P., Thinakram, N., Sivasany, A. and Sivanisan, S. (2008). Removal of Rhodamine B from aqueous solution by adsorption onto sodium montmorillonite. Journal of Hazardous Materials, **155**, 39-44.

Sohrabi, M. R. and Ghavami, M. (2008). Photocatalytic degradation of Direct Red 23 dye using UV/TiO_2: Effect of operational parameters. Journal of Hazardous Materials, **153 (3)**, 1235–1239.

Tahir, S. S and Rauf, N. (2006). Removal of cationic dye from aqueous solution by adsorption onto bentonite clay. Chemosphere, **63**, 1842-1848.

Tehrane-Bayha, A. R, Nikkar, H. N., Mahmoodi, N. M., Markazi, M. and Menger, F. M. (2011). The adsorption of cationic dyes onto Kalin: kinetic, isotherm and thermodynamic study. Desalination, **266**, 274-280.

Temkin, M. J. and Pyzhev, V. (1940). Kinetics of ammonia synthesis on promoted iron catalysts. ActaPhysiochim. URSS, **12**, 217–222.

Tsai, W. T., Chang, C. Y., Ing, C. H. and Chang, C. F. (2004). Adsorption of acid dyes from aqueous solution on activated bleaching earth. Journal of Colloid and Interface Science, 275, 72–78.

Vimonses, V., Lei, V., JinChris, B., Chow, V. and Saint, C. (2009). Adsorption of congo red by three Australian kaolins. Applied Clay Science, **43(3–4)**, 465–472.

Wang, H., Zheng, X. W., Qiang Su, J., Tian, Y., Xiong, X. J. and Zheng, T. L. (2009). Biological decolorization of the reactive dyes Reactive Black 5 by a novel isolated bacterial strain Enterobacter sp. EC3. Journal of Hazardous Materials, **171 (1–3)**, 654–659.

Wu, J. S., Liu, C. H., Chu, K. H. and Suen, S. Y. (2008). Removal of cationic dye methyl violet 2B from water by cation exchange membranes. Journal of Membrane Science, **309 (1–2)**, 239–245.

Yue, D., Jing, Y., Xia, C. and Jia, Y. (2011). Removal of neutral Red from aqueous solution by using modified bectorite. Desalination, **267,**9-15.

Zakhama, S., Dhaouadi, H. and M'Henni, F. (2011). Nonlinear modelisation of heavy metal removal from aqueous solution using Ulva lactuca algae. Bioresource Technology, **102 (2),** 786–796.